Molecular level investigation of the role of peptide interactions in the glyphosate analytics

Ashour A. Ahmed[1,2,*], Peter Gros[3], Oliver Kühn[1], Peter Leinweber[3]

[1] University of Rostock, Institute of Physics, D-18059 Rostock, Germany.

[2] University of Cairo, Faculty of Science, Department of Chemistry, 12613 Giza, Egypt.

[3] University of Rostock, Soil Science, D-18059 Rostock, Germany.

ashour.ahmed@uni-rostock.de

peter.gros@uni-rostock.de

oliver.kuehn@uni-rostock.de

peter.leinweber@uni-rostock.de

Corresponding author:

Ashour A. Ahmed

Email: ashour.ahmed@uni-rostock.de

Tel: +49-381-498-8982

Abstract

The detection of the herbicide glyphosate (GLP) in environmental samples is most often conducted after derivatizing the target molecule with the chromophore 9-fluorenylmethyloxycarbonyl chloride (FMOC-Cl). However, this method is sensitive to all primary and secondary amines, which can occur in the sample matrix as well. In order to quantify the interference of primary and secondary amines on GLP detection, we have used the oligo peptide pentaglycine (PG) as an example. PG has been added to the derivatization solution of GLP at different constant concentration levels and UV extinction coefficients have been determined. Data analysis supported by quantum chemical modeling of the GLP–PG, FMOC–GLP, and FMOC–PG complexation reactions facilitated the identification of two interfering impacts of PG on GLP derivatization: (i) increase of the signal due to its reaction with FMOC-Cl leading to an overestimation of GLP concentration and (ii) decrease of GLP recovery due to complex formation and therefore inhibition of GLP derivatization, which leads to an underestimation.

Keywords

FMOC-Cl, glyphosate, peptide, UV spectra, quantum chemical modelling

1. Introduction

Glyphosate (GLP) is the most commonly used herbicide worldwide. Although it is assumed that GLP is nearly immobile in soil (Borggaard and Gimsing, 2008) it was found in ground and surface waters (Aparicio et al., 2013) and recently in the Baltic Sea (Skeff et al., 2015). This emphasizes the need for reliable analytical methods to support the ongoing discussion of potential risks of unlimited GLP usage. The most frequently employed detection method for GLP is a chromatographic separation of the reversed phase and UV-spectrometric detection, often combined with mass-spectrometry (Ramirez et al., 2014). To this end, GLP has to be converted into a non-polar and UV-detectable form *via* a derivatization step. The standard derivatization method is the reaction of GLP with 9-fluorenylmethyloxycarbonyl chloride (FMOC-Cl) as described by Hanke et al. (2008).

The composition of environmental samples is generally complex, containing numerous diverse organic and inorganic constituents. These matrix components potentially interact with GLP in solution, e.g., by formation of stable complexes between GLP and multivalent cations (Freuze et al., 2007). Also, polar organic compounds containing phenolic, hydroxylic, carboxylic, and amino functional groups can form stable complexes with GLP *via* H-bond formation with the GLP phosphonic and carboxylic moieties (Gros et al., 2017). Primary and secondary amines such as peptides have the ability to interact with GLP (Castellino et al., 1989) as well as with the derivatization agent FMOC-Cl (Carpino and Han, 1972; Moye and Boning, 1979). This indicates that the GLP detection or quantification may be affected by peptides in the samples. The impact of possibly produced FMOC–peptide complexes can be avoided by chromatographic separation combined with mass-spectrometry (environmental samples with unknown concentration, Vreeken et al., 1998) or blank correction in the data evaluation (samples with known GLP concentrations such as those for sorption isotherms). However, possible interactions between peptides and GLP preventing the derivatization with FMOC-Cl cannot be corrected using the established analytical procedures. This is due to the lack of knowledge about concentration of GLP and peptides in environmental samples. Here, we hypothesize that the interaction of peptides with GLP can suppress the GLP reaction with FMOC-Cl, and this inhibiting effect on GLP derivatization may cause underestimations of GLP concentrations. Surprisingly, this possible disturbance of the GLP quantification has not been examined and described in the literature before.

The objective of the present study was to scrutinize possible inhibition effects at a molecular level by investigating the GLP derivatization with FMOC-Cl in the presence of an oligopeptide such as pentaglycine (PG). Specifically, the interactions between GLP and PG, FMOC-Cl and GLP, and FMOC-Cl and PG will be explored experimentally by calibration studies and theoretically by quantum chemical modeling.

2. Materials and Methods

2.1. Chemicals and Calibration Solutions

GLP (CAS: 1071-83-6), FMOC-Cl (CAS: 28920-43-6), dichlormethane (CAS: 75-09-2) and sodium tetraborate decahydrate (CAS: 1330-43-4) were purchased from Sigma Aldrich. PG (CAS: 7093-67-6) was purchased from Fluorochem Ldt. Hydrochloric acid and sodium hydroxide were used for pH adjustment of GLP and PG solutions. Concentration levels of single components GLP and PG were prepared in the range of 2.96 to 94.67 mmol/L by diluting GLP and PG from stock solutions. The GLP calibration solution was also prepared in the presence of three distinct levels of PG (2.96, 23.67, 94.67 mmol/L). Four replicates per concentration level were prepared.

2.2. Derivatization and UV-detection

The method proposed by Waiman et al. (2012) for complex environmental samples like soil was used for GLP and PG derivatization. Briefly, 0.5 mL borate buffer solution (pH 9) was added to 4 mL of sample solution. Next, an excess concentration of FMOC-Cl (0.5 mL, c = 1 g/L; dissolved in acetonitrile) was added. After vigorously shaking the derivatization solution was allowed to react for 2 h with occasionally shaking. Subsequently, by-products of FMOC-Cl (FMOC-OH) were removed by extracting with 4 mL dichloromethane. The mixture was centrifuged (10 min., 1558 x g) to separate the two phases. The supernatant aqueous phases of each derivatization solution were used for UV/Vis spectroscopy at λ = 264 nm (Specord200, Analytik Jena AG, 07745 Jena, Germany). The averaged signals of the calibration series of the respective analyte were corrected by subtracting the signal intensity of the blank level containing no analyte. In this way effects on signal intensity resulting from matrix constituents were eliminated.

2.3. Quantum Chemical Modeling

The interaction between GLP and PG was simulated through 1:1 complex formation between them, i.e. 1GLP + 1PG → GLP–PG complex. Here, different initial geometries for this complex were constructed by selecting the expected preferential binding situations between GLP and PG. The aqueous solution around the complex was simulated by introducing an implicit treatment through the conductor-like polarizable continuum model (CPCM, Cossi et al., 2003) Full geometry optimization, using CPCM, was performed for the complexes as well as for the individual species (GLP and PG). The calculations have been performed using density functional theory (DFT) implemented in the Gaussian09 program package (Frisch et al., 2013). Specifically, the B3LYP hybrid functional (Becke, 1988; Lee et al., 1988) combined with the 6-311++G(d,p) basis set (Hehre et al., 1972) and Grimme's D3 dispersion correction (Grimme et al., 2011) has been applied. The basis set superposition error (BSSE) has been corrected using the counterpoise scheme (Jansen and Ros, 1969). For more details about the different methods of computational chemistry and their application to soil science, see also Kubicki (2016).

For the complexation reaction, 1GLP + 1PG → GLP–PG complex, the reaction energy (∆E) is calculated as follows:

$$\Delta E = E_{GLP-PG\ complex} - (E_{GLP} + E_{\mathrm{PG}}) \quad (1)$$

where, $E_{GLP-PG\ complex}$, E_{GLP}, and E_{PG}, are the electronic energies of the GLP–PG complex, GLP, and PG, respectively. Similarly, the corresponding reaction free energy (∆G) is calculated by including the zero point energy and thermal correction to the Gibbs free energy.

The derivatization reactions of FMOC-Cl with GLP as well as with PG have been simulated at the same level of theory. For PG, we have considered five possibilities for the 1:1 FMOC–PG derivatization reaction according to the five amino groups (for details see Figure S1 and Figure S2 in the Supplemental Material). For the derivatization reaction, 1FMOC-Cl + 1GLP(PG) → FMOC–GLP(PG) complex + HCl, the reaction energy (∆E) is calculated as follows:

$$\Delta E = E_{FMOC-GLP(PG)\ complex} + E_{HCl} - \left(E_{FMOC-Cl} + E_{\mathrm{GLP(PG)}}\right) \quad (2)$$

where, $E_{FMOC-GLP(PG)\ complex}$, E_{HCl}, $E_{FMOC-Cl}$, and $E_{GLP(PG)}$ are the electronic energies of the FMOC–GLP or FMOC–PG complex, HCl, FMOC-Cl, and GLP or PG,

respectively. Moreover, UV spectra for FMOC-Cl as well as for the FMOC–GLP and FMOC–GP complexes have been calculated using linear response time-dependent DFT.

3. Results and Discussion

3.1. Quantum Chemical Modeling

The optimized geometry for the GLP–PG complex in Figure 1a indicates a strong interaction between GLP and PG. This is due to the high polarity of GLP and PG, which contain several polar functional groups (phosphonic, amino, carboxylic, and amide). The GLP–PG complex formation involves multiple intermolecular interactions. Especially, PG forms a cavity around GLP in addition to formation of intermolecular and intramolecular H-bonds (HBs) and proton transfer. Four intermolecular HBs are observed between PG and the GLP phosphonic and carboxylic functional groups. Here, the GLP phosphonic group is involved in three HBs with O---H bond lengths of 1.53, 1.57, and 1.75 Å. The GLP carboxylic group participated with one weaker HB with O---H bond length of 1.95 Å. This indicates a stronger interaction for the GLP phosphonic group than the corresponding carboxylic one. Moreover, the calculated reaction energy (–38.8 kcal/mol) and reaction free energy (–17.6 kcal/mol) indicates that the GLP–PG complex is strongly bound, thermally stable, and can be formed spontaneously. This already hints at the possibility of masking of GLP by peptides in environmental samples.

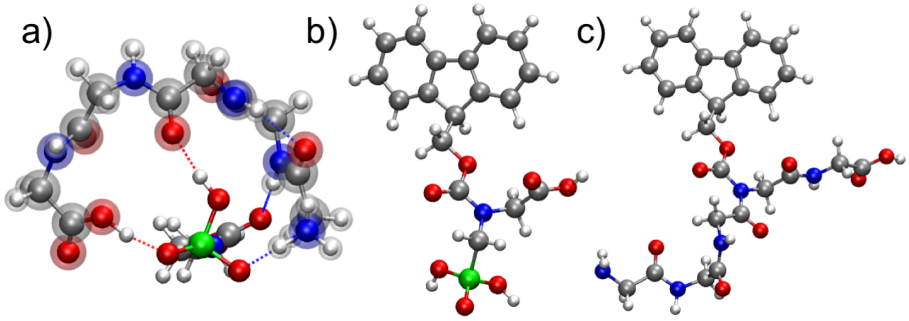

Figure 1: Optimized geometries of the GLP–PG (a), FMOC–GLP (b), and FMOC–PG complexes (c) at the DFT/B3LYP/D3/6–311++G(d.p) level of theory and using the CPCM model. For the GLP–PG complex, PG atoms are surrounded by transparent spheres for better visualization of the complex formation. White, gray, blue, red, and green colors are corresponding to H, C, N, O, and P atoms, respectively.

In order to investigate the competition between PG and FMOC-Cl regarding their interaction with GLP, the FMOC–GLP derivatization reaction has been simulated. The calculated reaction energy and free energy for this reaction is –18.8 and –16.3 kcal/mol, respectively (for more details, see Figure 1b and Table S1). Thus, the

reaction is exothermic and can occur spontaneously. Compared to energies of the GLP–PG complex, one can observe that GLP can interact with peptides *stronger* than with FMOC-Cl.

The interaction of FMOC-Cl with PG has been simulated through a similar derivatization reaction (see Figure 1c and Figure. S2). The results indicate complex formation between FMOC-Cl and PG at five interaction sites (five amino groups), the most stable one occurs at the PG primary amino group. For this complex, the calculated reaction energy and free energy for the FMOC–PG derivatization reaction is –13.9 and –11.8 kcal/mol, respectively (see Table S1). Similar to the FMOC–GLP case, these reaction energies also point to a spontaneous complex formation reaction between FMOC-Cl and PG. This indicates that both GLP and PG can form complexes with FMOC-Cl of similar binding strength.

The calculated UV spectra shown in Figure 2, for FMOC-Cl and its complexes with GLP and PG, reveal two peaks at 219 nm and 275 nm. This comes in a good agreement with the experimentally observed UV peaks for FMOC-Cl (Catrinck et al., 2014). For FMOC-Cl, the peak at 275 nm corresponds mainly to π(fluorene ring) → π*(fluorene ring) electronic transitions while the peak at 219 nm is a result of combination the π(fluorene ring) → π*(fluorene ring) and π(fluorene ring) → σ*(C-Cl) electronic transitions (for more details, see Figures S3-S5). For this reason, the peak at 275 nm is not influenced by the binding of GLP and PG, while the one at 219 nm shows a reduced intensity for the complex. Most importantly, however, is the observation that there is essentially no effect of GLP and PG binding on the spectrum. Thus, based on the extinction coefficient one cannot discriminate between the two species.

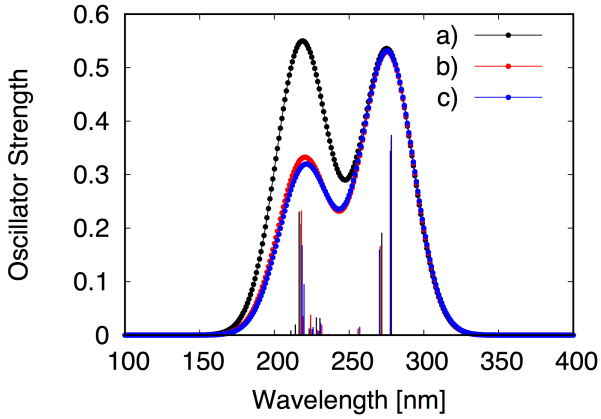

Figure 2. Calculated UV spectra with their electronic transitions for FMOC-Cl (a) and its complexes with GLP (b) and PG (c) at the TD-DFT/B3LYP/6–311++G(d.p)/ CPCM level of theory.

3.2. Calibration Experiments

The calibration curves of the individual species GLP and PG in aqueous solution show different extinctions for each molar concentration (Figure 3). The calibration curves show an approximately linear behavior (R^2 = 0.997 for GLP and R^2 = 0.994 for PG) within the measured concentration range. The slope of the calibration curve for PG (0.0024 L/mmol) is almost twice of that for GLP (0.0013 L/mmol). Since the calculated extinction is the same for both species, this doubled signal intensity of PG in comparison to GLP at equal molar concentrations indicates that the number of FMOC-Cl chromophores per one complexed PG molecule is twice of that per one complexed GLP molecule. Since GLP can react with only one FMOC-Cl molecule, this means that one PG molecule can react with two FMOC-Cl molecules. This is in accord with the quantum chemical results, indicating different sites for FMOC-Cl to PG binding (see also Figure S2).

For a sample containing GLP and known PG concentration, a standard blank subtraction for calibration of GLP can correct the increased extinction coming from the FMOC–PG complex signal. Of course, this only holds true if these reactions are independent of each other and there is no interference with the remaining matrix. In order to check this GLP calibration curves have been measured in the presence of constant concentrations of PG as shown in Figure 4. Here we observe a decreasing UV signal with increasing the PG concentration, i.e. slope changes like 0.0023 L/mmol (2.96 $mmol_{PG}$/L) < 0.0018 L/mmol (23.67 $mmol_{PG}$/L) < 0.0011 L/mmol (96.64 $mmol_{PG}$/L). This observation is readily explained using the quantum chemical results. The strong binding of GLP and PG reduces the availability of GLP for derivatization and thus for reaction with the FMOC-Cl UV sensor. Thus, the 1:1 complex formation reaction between GLP and PG is an example for the matrix interference.

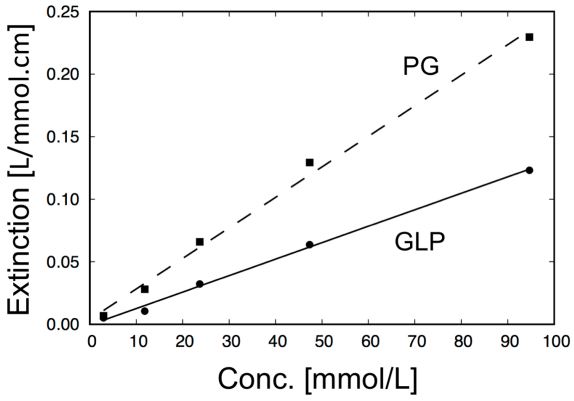

Figure 3: Calibration curves separately determined for GLP and PG.

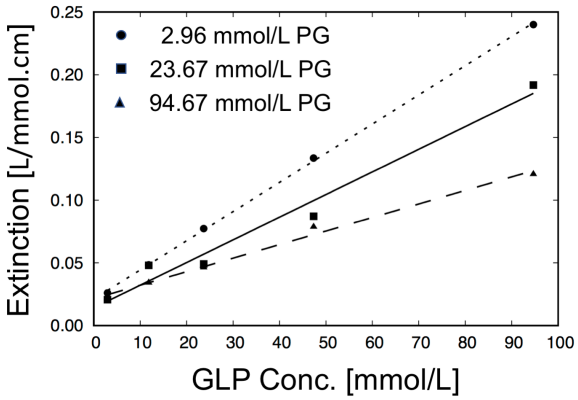

Figure 4: Calibration curves of GLP in the presence of different concentrations of PG. Note that a blank correction for PG has been applied.

3.3. Implications for Soil Samples

Soil samples have unknown concentrations of GLP and PG (as well as other primary and secondary amines which are present in soil in a range of 9 to 24 mg g^{-1} of humic substances, Ramunni et al., 1985) which likely interfere with each other, a blank cannot be defined and blank correction is impossible. Since the non-specific nature of FMOC-Cl with respect to GLP and PG is well-known (Moye and Boning, 1979), calibration experiments with chromatographic separation and mass-spectrometric detection have been performed. For instance, calibration experiments with chromatographic separation yielded recovery rates of 70 to 80 % (Roseboom and Berkhoff, 1982) and those with mass-spectrometric detection of FMOC–GLP molecules yielded a recovery rate of about 67% (Ramirez et al., 2014). Similarly, the use of ^{13}C and ^{15}N isotopic labelled GLP (GLP_{ISO}) standards in combination with chromatographic separation and mass-spectrometric detection led to a recovery of 80% (Grey et al., 2001). In other words, these recovery rates indicate 33% to 20% of undetermined GLP form. In view of the present findings (Fig. 4), these observations can be explained by formation of stable complexes between GLP and matrix constituents (such as peptides) that inhibit the derivatization of GLP by FMOC-Cl. The use of isotopic labelled standards may not correct these effects since sample GLP, parts of which previously reacted with sample peptides, and added GLP_{ISO} do not exist in the same free form as it is required for a uniform derivatization.

4. Conclusion

In conclusion, these model experiments and quantum chemical modeling reveal a strong interaction of GLP and PG in solution. Both species react similar with FMOC-Cl and additionally interfere with each other thus are likely to inhibit the GLP derivatization reaction. As a consequence, two competing effects can occur in soil samples. First, the presence of peptides (or other species binding to FMOC-Cl) may lead to an overestimation of the GLP concentration. Second, the complexation of GLP with peptides (or other species binding to GLP, e.g. metal ions) may cause an underestimation of the GLP concentration. In soil samples the magnitudes of these competing effect are not known and even a cancelation of both effects could be possible. This makes an accurate quantitative determination of GLP in such samples using FMOC-Cl complicated. In forthcoming studies these preliminary results must be confirmed with real soil samples and thus the effects of the reactions shown in the present study on the state-of-the-art GLP detection methods (e.g. LC/MSMS) investigated.

Acknowledgements

The modeling part of this work has been performed within the InnoSoilPhos-project (http://www.innosoilphos.de/default.aspx), funded by the German Federal Ministry of Education and Research (BMBF) in the frame of the BonaRes-program (No. 031A558). Peter Gros acknowledges a PhD-grant from the state of Mecklenburg-Western Pommeria. This research was conducted within the scope of the Leibniz ScienceCampus Phosphorus Research Rostock.

References

Aparicio VC, De Gerónimo E, Marino D, Primost J, Carriquiriborde P, Costa JL. Environmental fate of glyphosate and aminomethylphosphonic acid in surface waters and soil of agricultural basins. Chemosphere 2013;93:1866–73. doi:10.1016/j.chemosphere.2013.06.041.

Becke AD. Density-functional exchange-energy approximation with correct asymptotic behavior. Phys Rev A 1988;38:3098–100. doi:10.1103/PhysRevA.38.3098.

Borggaard OK, Gimsing AL. Fate of glyphosate in soil and the possibility of leaching to ground and surface waters: a review. Pest Manag Sci 2008;64:441–56. doi:10.1002/ps.1512.

Carpino LA, Han GY. 9-Fluorenylmethoxycarbonyl amino-protecting group. J Org Chem 1972;37:3404–9. doi:10.1021/jo00795a005.

Castellino S, Leo GC, Sammons RD, Sikorski JA. Phosphorus-31, nitrogen-15, and carbon-13 and NMR of glyphosate: comparison of pH titrations to the herbicidal dead-end complex with 5-enolpyruvoylshikimate-3-phosphate synthase. Biochemistry (Mosc) 1989;28:3856–68. doi:10.1021/bi00435a035.

Catrinck TCPG, Dias A, Aguiar MCS, Silvério FO, Fidêncio PH, Pinho GP. A Simple and Efficient Method for Derivatization of Glyphosate and AMPA Using 9-Fluorenylmethyl Chloroformate and Spectrophotometric Analysis. J Braz Chem Soc 2014. doi:10.5935/0103-5053.20140096.

Cossi M, Rega N, Scalmani G, Barone V. Energies, structures, and electronic properties of molecules in solution with the C-PCM solvation model. J Comput Chem 2003;24:669–81. doi:10.1002/jcc.10189.

Freuze I, Jadas-Hecart A, Royer A, Communal P-Y. Influence of complexation phenomena with multivalent cations on the analysis of glyphosate and aminomethyl phosphonic acid in water. J Chromatogr A 2007;1175:197–206. doi:10.1016/j.chroma.2007.10.092.

Frisch MJ, Trucks GW, Schlegel HB, Scuseria GE, Robb MA, Cheeseman JR, et al. Gaussian 09 Revis D01 Gaussian Inc Wallingford CT 2013.

Grey L, Nguyen B, Yang P. Liquid chromatography/electrospray ionization/isotopic dilution mass spectrometry analysis of n-(phosphonomethyl) glycine and mass spectrometry analysis of aminomethyl phosphonic acid in environmental water and vegetation matrixes. J AOAC Int 2001;84:1770–80.

Grimme S, Ehrlich S, Goerigk L. Effect of the damping function in dispersion corrected density functional theory. J Comput Chem 2011;32:1456–65. doi:10.1002/jcc.21759.

Gros P, Ahmed A, Kühn O, Leinweber P. Glyphosate binding in soil as revealed by sorption experiments and quantum-chemical modeling. Sci Total Environ 2017;586:527–35. doi:10.1016/j.scitotenv.2017.02.007.

Hanke I, Singer H, Hollender J. Ultratrace-level determination of glyphosate, aminomethylphosphonic acid and glufosinate in natural waters by solid-phase extraction followed by liquid chromatography–tandem mass spectrometry: performance tuning of derivatization, enrichment and detection. Anal Bioanal Chem 2008;391:2265–76. doi:10.1007/s00216-008-2134-5.

Hehre WJ, Ditchfield R, Pople JA. Self—Consistent Molecular Orbital Methods. XII. Further Extensions of Gaussian—Type Basis Sets for Use in Molecular Orbital Studies of Organic Molecules. J Chem Phys 1972;56:2257–61. doi:10.1063/1.1677527.

Jansen HB, Ros P. Non-empirical molecular orbital calculations on the protonation of carbon monoxide. Chem Phys Lett 1969;3:140–3. doi:10.1016/0009-2614(69)80118-1.

Kubicki JD, editor. Molecular modeling of geochemical reactions: an introduction. Chichester, West Sussex, United Kingdom: Wiley; 2016.

Lee C, Yang W, Parr RG. Development of the Colle-Salvetti correlation-energy formula into a functional of the electron density. Phys Rev B 1988;37:785–9. doi:10.1103/PhysRevB.37.785.

Moye HA, Boning AJ. A Versatile Fluorogenic Labelling Reagent for Primary and Secondary Amines: 9-Fluorenylmethyl Chloroformate. Anal Lett 1979;12:25–35. doi:10.1080/00032717908082516.

Ramirez CE, Bellmund S, Gardinali PR. A simple method for routine monitoring of glyphosate and its main metabolite in surface waters using lyophilization and LC-FLD+MS/MS. Case study: canals with influence on Biscayne National Park. Sci Total Environ 2014;496:389–401. doi:10.1016/j.scitotenv.2014.06.118.

Ramunni A, Scialdone R, Felleca D. Analytical problems in determining peptide nitrogen in the humic fractions of three Italian soils. Org Geochem 1985;8:87–93. doi:10.1016/0146-6380(85)90056-7.

Roseboom H, Berkhoff CJ. Determination of the herbicide glyphosate and its major metabolite aminomethylphosphonic acid by high-performance liquid chromatography after fluorescence labelling. Anal Chim Acta 1982;135:373–7. doi:10.1016/S0003-2670(01)93923-6.

Skeff W, Neumann C, Schulz-Bull DE. Glyphosate and AMPA in the estuaries of the Baltic Sea method optimization and field study. Mar Pollut Bull 2015;100:577–85. doi:10.1016/j.marpolbul.2015.08.015.

Vreeken R., Speksnijder P, Bobeldijk-Pastorova I, Noij TH. Selective analysis of the herbicides glyphosate and aminomethylphosphonic acid in water by on-line solid-phase extraction–high-performance liquid chromatography–electrospray ionization mass spectrometry. J Chromatogr A 1998;794:187–99. doi:10.1016/S0021-9673(97)01129-1.

Waiman CV, Avena MJ, Garrido M, Fernández Band B, Zanini GP. A simple and rapid spectrophotometric method to quantify the herbicide glyphosate in aqueous media. Application to adsorption isotherms on soils and goethite. Geoderma 2012;170:154–8. doi:10.1016/j.geoderma.2011.11.027.

Supplementary Material

Molecular level investigation of the role of peptide interactions in the glyphosate analytics

Ashour A. Ahmed[1,2,*], Peter Gros[3], Oliver Kühn[1], Peter Leinweber[3]

[1] University of Rostock, Institute of Physics, D-18059 Rostock, Germany.

[2] University of Cairo, Faculty of Science, Department of Chemistry, 12613 Giza, Egypt.

[3] University of Rostock, Soil Science, D-18059 Rostock, Germany.

ashour.ahmed@uni-rostock.de

peter.gros@uni-rostock.de

oliver.kuehn@uni-rostock.de

peter.leinweber@uni-rostock.de

Figures

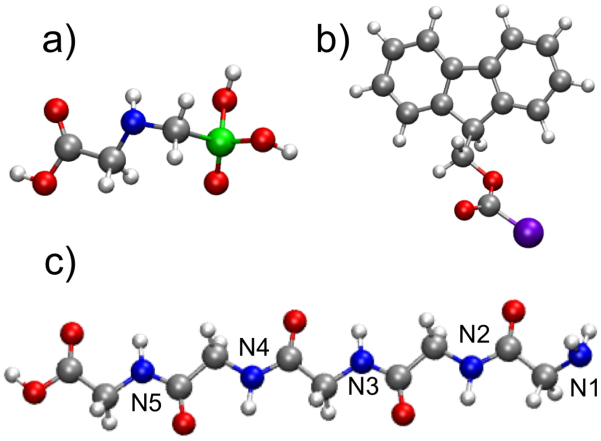

Figure S1. Optimized geometries of GLP (a), FMOC-Cl (b), and PG (c) at the B3LYP/D3/6–311++G(d.p) level of theory and using the CPCM model. White, gray, blue, red, green, and violet colors are corresponding to H, C, N, O, P, and Cl atoms, respectively.

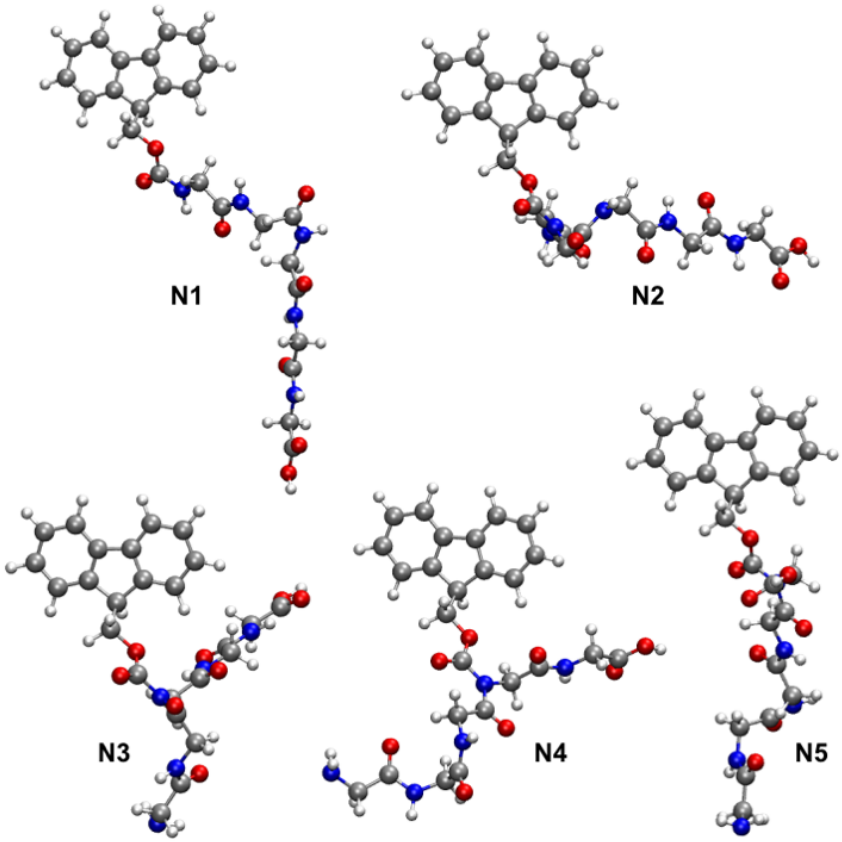

Figure S2. Optimized geometries of the FMOC–PG complexes at the B3LYP/D3/6–311++G(d.p) level of theory and using the CPCM model. Here the FMOC-Cl derivatization reactions take place at five different PG amino groups, primary amino group (N1) and four secondary amino groups (N2 to N5 ordered from the PG amino group to the PG carboxylic group). White, gray, blue, red, and green colors are corresponding to H, C, N, O, and P atoms, respectively.

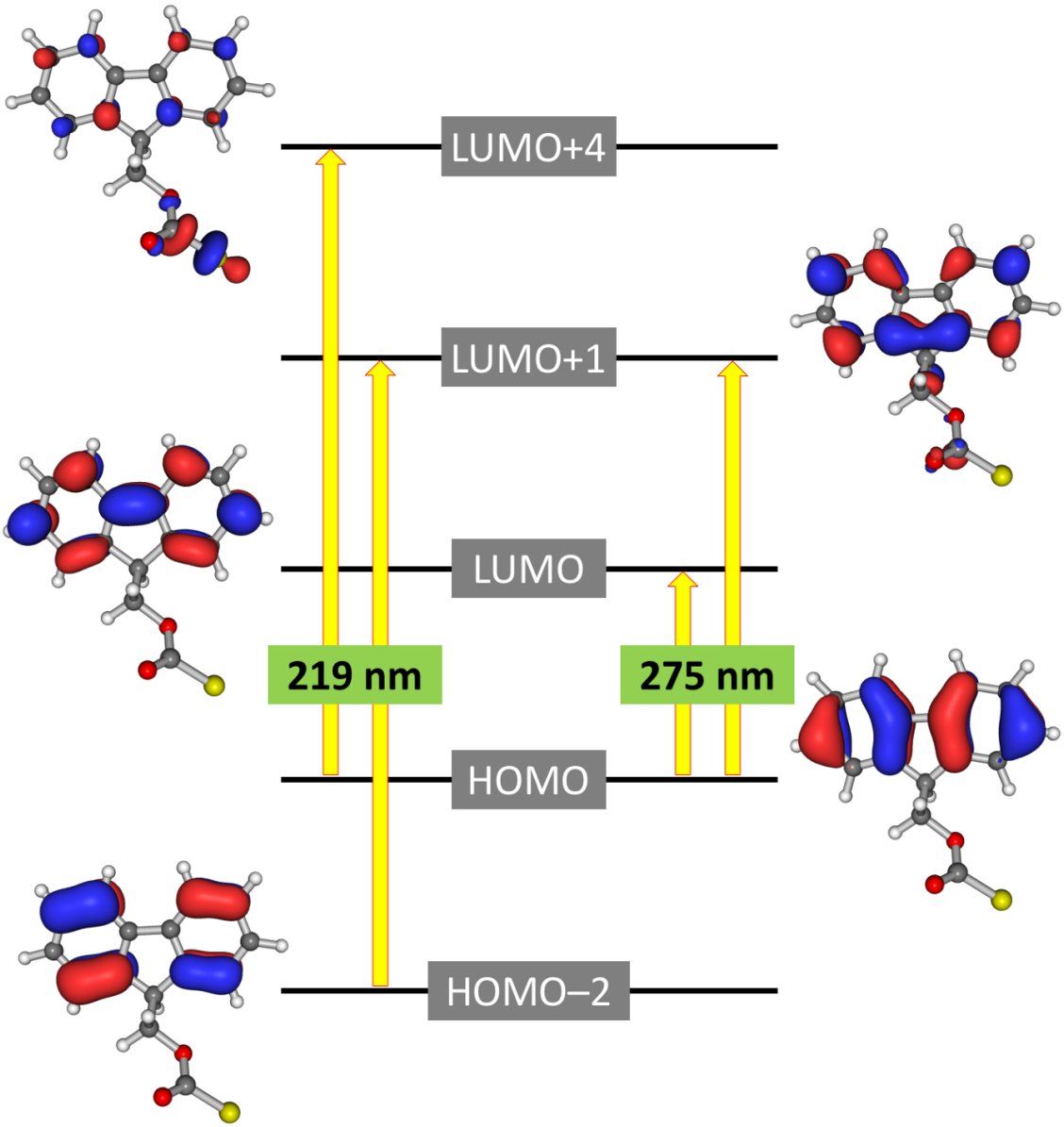

Figure S3. Possible electronic transitions from the highest occupied molecular orbitals (HOMOs) to the lowest unoccupied molecular orbitals (LUMOs) for FMOC-Cl calculated at the TD-DFT/B3LYP/6–311++G(d.p)/ CPCM level of theory.

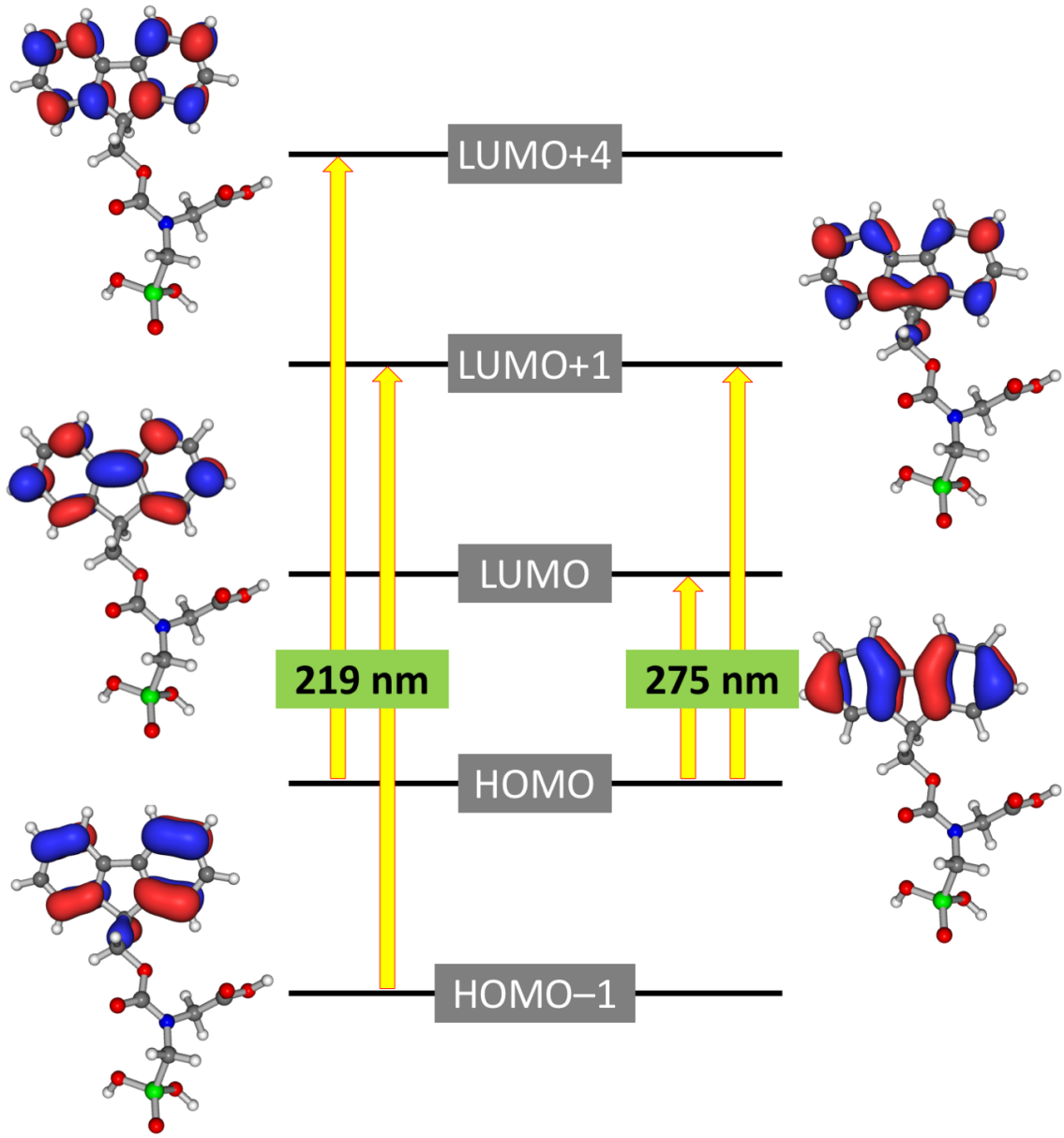

Figure S4. Possible electronic transitions from the highest occupied molecular orbitals (HOMOs) to the lowest unoccupied molecular orbitals (LUMOs) for the FMOC-GLP complex calculated at the TD-DFT/B3LYP/6–311++G(d.p)/ CPCM level of theory.

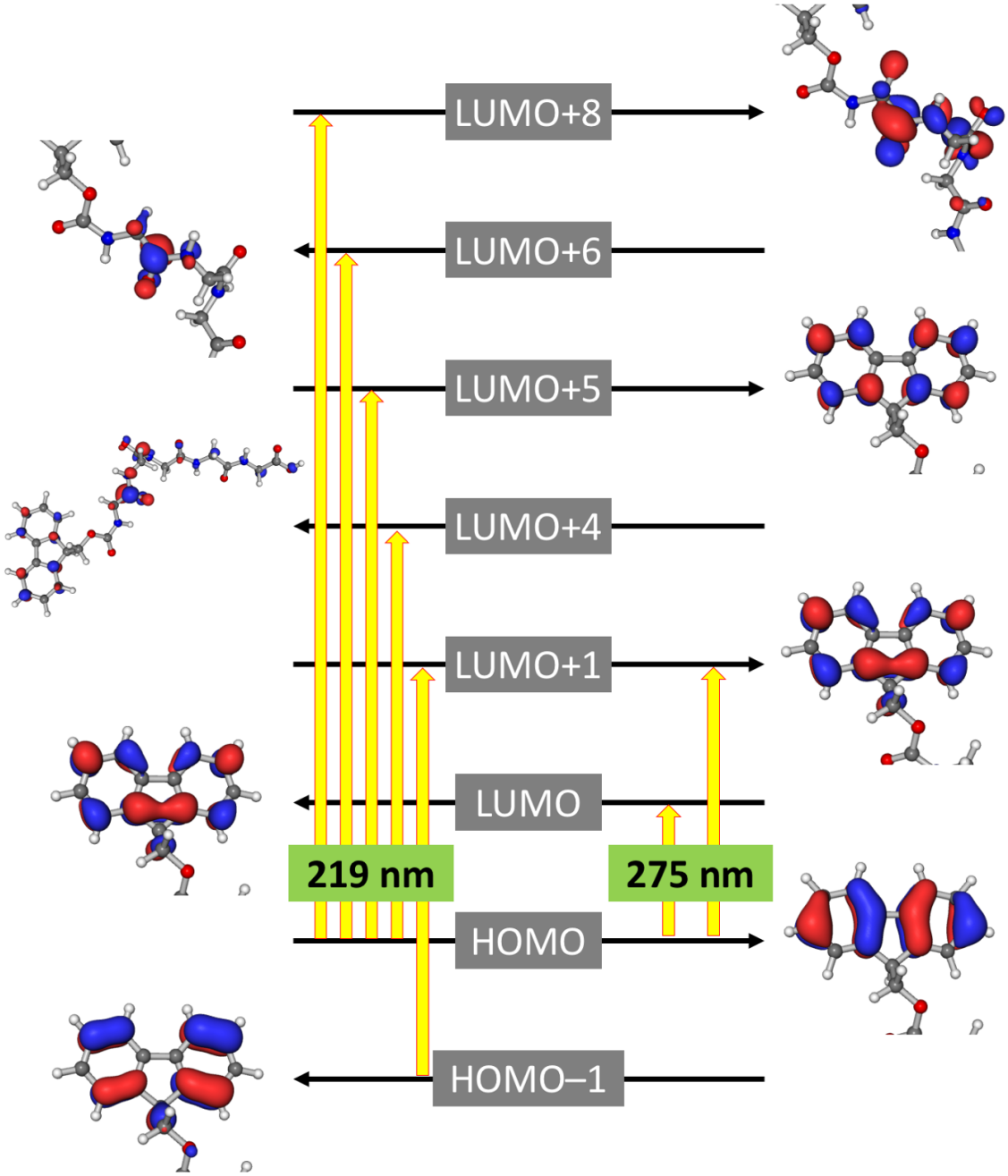

Figure S5. Possible electronic transitions from the highest occupied molecular orbitals (HOMOs) to the lowest unoccupied molecular orbitals (LUMOs) for the FMOC-PG complex calculated at the TD-DFT/B3LYP/6–311++G(d.p)/ CPCM level of theory.

Table

Table S1. Calculated reaction energies and free energies at the B3LYP/D3/6–311++G(d.p) level of theory and using the CPCM model for the derivatization reactions of FMOC-Cl with GLP and with PG at five different PG amino groups (primary amino group (N1) and four secondary amino groups (N2 to N5 ordered from the PG amino group to the PG carboxylic group)).

	ΔE (kcal/mol)	ΔG (kcal/mol)
FMOC-GLP	-18.8	-16.3
FMOC-PG (N1)	-13.9	-11.8
FMOC-PG (N2)	-1.0	3.1
FMOC-PG (N3)	-1.1	1.6
FMOC-PG (N4)	-2.9	0.1
FMOC-PG (N5)	-2.1	1.6